

Asymmetric phosphorus incorporation in homoepitaxial P-doped (111) diamond revealed by photoelectron holography

T. Yokoya,^{,†,‡} K. Terashima,^{†,#} A. Takeda,[‡] T. Fukura,[‡] H. Fujiwara,[‡] T. Muro,^{||} T. Kinoshita,^{||}
H. Kato,[§] S. Yamasaki,[§] T. Oguchi,[#] T. Wakita,[†] Y. Muraoka,^{†,‡} and T. Matsushita^{*,||}*

[†]Research Institute for Interdisciplinary Science (RIIS), Okayama University, Okayama 700-3537, Japan

[‡]Graduate School of Science and Technology, Okayama University, Okayama 700-3537, Japan

^{||}Japan Synchrotron Radiation Research Institute (JASRI)/SPring-8, 1-1-1 Kouto, Sayo, Hyogo 679-5198, Japan

[§]Energy Technology Research Institute, National Institute of Advanced Industrial Science and Technology (AIST), Tsukuba Center 2, Tsukuba, Ibaraki 305-8568, Japan

[#]Institute of Scientific and Industrial Research, Osaka University, 8-1 Mihogaoka, Ibaraki, Osaka 567-0047, Japan

ABSTRACT: Diamond has two crystallographically inequivalent sites in the unit cell. In doped diamond, dopant occupation in the two sites is expected to be equal. Nevertheless, preferential

dopant occupation during growth under non-equilibrium conditions is of fundamental importance, for example, to enhance the properties of nitrogen-vacancy (N-V) centres; therefore, this is a promising candidate for a qubit. However, the lack of suitable experimental techniques has made it difficult to study the crystal- and chemical-site-resolved local structures of dopants. Here, we confirm the identity of two chemical sites with asymmetric dopant incorporation in the diamond structure, via the photoelectron holography (PEH) of heavily phosphorus (P)-doped diamond prepared by chemical vapor deposition. One is substitutionally incorporated P with preferential site occupations and the other can be attributed to a PV split vacancy complex with preferential orientation. The present study shows that PEH is a valuable technique to study the local structures around dopants, with a resolution of crystallographically inequivalent but energetically equivalent sites/orientations. Such information provides strategies to improve the properties of dopant related-complexes in which alignment is crucial for sensing of magnetic field or quantum spin register using N-V centres in diamond.

KEYWORDS: Dopant local structure, asymmetric dopant incorporation, substitutional doping, dopant-vacancy complex, diamond, photoelectron holography

The incorporation of dopant atoms, vacancies, and dopant-related complexes (known as point defects) into semiconductors is a method to not only control conducting properties but also induce new functionalities, like optical properties, derived from dopant-vacancy complexes¹. Diamond, due to its extraordinary properties that can be used for several applications, synthesis of high-quality single crystal diamond, by controlling the crystal orientation, synthesis process, and doping, has been a popular and important research subject in the field of the materials

science²⁻⁹. Recently, the demand for understanding point defects, especially in diamond, is increasing, as nitrogen-vacancy (N-V) centres can be used for quantum technology, including quantum metrology and information processing and communications¹⁰⁻¹². Interestingly, control of the alignment of N-V centres for enhancing the properties has been reported in doped diamond synthesized by chemical vapour deposition (CVD)¹³⁻¹⁵. In previous studies¹⁶, the mechanism of the alignment has been explained theoretically based on the preferential incorporation of a nitrogen atom at one of the two crystallographically inequivalent sites¹⁷ in diamond during CVD.

However, experimental confirmation of the crystal site occupation of substitutionally incorporated dopants in the diamond structure is difficult because the two crystal sites are energetically equivalent. Optical spectroscopy and electron paramagnetic resonance spectroscopy are conventional techniques to study the characteristics of point defects in diamond¹⁸, but are applicable for deducing local structures. Rutherford backscattering spectrometry using channelling techniques¹⁹ can provide the location of interstitial dopants, but not that of substitutional dopants. Extended X-ray absorption fine structure (EXAFS) analysis provides the bond length to and coordination number of neighbouring atoms around selected elements, but without information on the direction of neighbouring atoms²⁰. Scanning transmission electron microscopy can be used to detect the site in principle²¹, because it can provide the three-dimensional (3D) local structure. However, it cannot be used for determining light elements or vacancies.

Photoelectron holography (PEH) is promising for determining the 3D local structure around a dopant atom²², with chemical-site and crystal-site selectivity. In the core-level photoelectron angular distribution, i.e. the photoelectron hologram, an interference pattern between two types of photoelectron waves is involved, one of which comes directly from the atom (emitter) and the

other is scattered by neighbouring atoms (scatterer) (Fig. 1). Since the photoelectron hologram reflects the local crystal structure around the atom where photo-excitation takes place, a 3D atomic image can be directly reconstructed from the photoelectron hologram using a developed reconstruction algorithm²³. Recently, PEH using third-generation synchrotron light has facilitated the observation of the local structure of dopant atoms in impurity-doped semiconductors^{24,25}. For the preferential incorporation of dopant atoms, there is a pioneering study on the local structure of boron-doped sites in heavily B-doped diamond²⁶; however, it was a chemical-site-integrated study and the reconstruction of atomic images was not performed.

In this study, we performed the PEH of heavily phosphorous-doped diamond synthesized via microwave plasma-assisted chemical vapor deposition (MPCVD) to experimentally determine the local structure of two chemical sites.

The image on the left-hand side in Fig. 2(a) shows the measured C 1s photoelectron hologram of heavily P-doped homoepitaxial (111) diamond. There are intense regions around particular parts that correspond to the [111] and [110] directions, and also several dark and bright lines. The higher-intensity spots are forward focusing peaks (FFP), which indicate the directions of the scatterer with respect to the emitter, because the scatterer atoms play the role of a convex lens. The dark lines are Kikuchi lines that reflect long-range structural coherence. In the diamond structure (Fig. 2(f) (left)), there are two crystallographically inequivalent sites at (0,0,0) and (1/4,1/4,1/4), termed A and B sites, respectively. While a carbon atom in the B site has three bonds directed diagonally upward, a carbon atom in the A site has three bonds directed diagonally downward. The photoelectron hologram is the sum of the two holograms viewed from the A and B sites. The cross sections of the reconstructed atomic images cut by planes perpendicular to [001] at $z = 0, 0.89, 1.78, \text{ and } 2.67 \text{ \AA}$ for the A site, which also correspond to the

planes for the B site (Fig. 2(f) (right)), are shown as [P1], [P2], [P3], and [P4], respectively, in Fig 2(b). The reconstructed images are located at the expected positions of carbon atoms (larger (smaller) circles viewed from A (B) site) in the diamond lattice. The calculated photoelectron hologram (right side of Fig. 2(a)) also reproduces the experiment reasonably well.

The measured P 2p core-level spectra are shown in Fig. 2(g). The spectra are reproduced with two components having a spin orbit partner (value of splitting is 0.84 eV). Here, higher and lower binding-energy components are labelled as α and β , respectively. We found that the two components exhibit similar angular dependence with a small variation, indicating that the two components may have a common depth profile. We also found good correspondence of the binding energies with those of two bulk components in a previous work²⁷. The spectral ratio α to β is 30:70, which is different from that obtained in a previous study²⁷. Since we found that the ratio depends on surface treatments before photoemission measurements (surface treated with hydrogen plasma (present study) or as-deposited surface (previous study)), we attribute the different ratio to the difference in surface condition. Subsequently, all the angular-dependent P 2p spectra were fitted by the two components to obtain the holograms. The images on the left-hand side in Figs. 2 (c) and (d) show the photoelectron holograms of the α and β components, respectively. The patterns are distinct, indicating that the local crystal structures around the P atoms of the two chemical sites are different.

The hologram pattern of component α rather resembles that of C 1s (Fig. 2(a)), suggesting that the P atoms of the chemical site are substitutionally incorporated into the diamond lattice. Indeed, in Fig. 2(e), the reconstructed 3D atomic images are observed at the locations expected for the carbon atoms in the diamond crystal. The substitutional incorporation of P atoms for P-doped diamond ($n_p \sim 4 \times 10^{19} \text{ cm}^{-3}$) was previously reported using Rutherford backscattering²⁸.

Interestingly, we found that the reconstructed atomic images are observed only at expected atomic positions viewed from the A site (larger circles of [P2] and [P4] of Fig. 2(e)). This indicates that the P atoms are preferentially incorporated into the A site of the diamond lattice, i.e., asymmetric dopant incorporation has occurred. We fitted the experimental hologram using two simulated holograms of the A and B sites, and found the occupancy to be 82% of the A site and 18% of the B site (Supporting Information). The simulated hologram obtained using the occupation ratio is shown in the right-hand-side image in Fig. 2(c); it reproduces the experimental hologram well. We will discuss the preferential incorporation later.

Regarding component β , we found that a simulated hologram considering contributions of PV^V oriented to [111] and PV^H oriented to other directions with occupancies of 69% and 31%, respectively, reproduces the experimental hologram (right side of Fig. 2(d)). This suggests that the PV split vacancy complex (PVSVC), where a P atom occupies the centre of two vacancies (Fig. 3), is the most probable candidate. Notably, the occupancy deviates from the geometrically expected value ($PV^V:PV^H=50:50$), providing evidence for the preferential orientation of the P-V complex. Although a recent EXAFS study reported the interstitial site occupation of P atoms²⁹, the simulated hologram therein did not explain the main features of the experimental hologram (Supporting Information).

The possibility of the PVSVC in P-doped diamond has been discussed theoretically³⁰. Since the PVSVC forms empty in-gap states, the valence state should be $[PV]^{-1}$ with spin $S = 0$, and no internal optical transitions are expected. This has made it difficult to reveal the identity from spectroscopic studies. The present PEH observed the ‘hidden’ P-complex in P-doped diamond by utilizing the characteristic ability of the method. Since the PVSVC compensates the electron

carrier induced by substitutional P and thus reduces the doping efficiency, reducing the PVSVC is an appropriate strategy for improving the doping efficiency.

The present PEH study reveals asymmetric P dopant incorporation, i.e. the preferential incorporation of P atoms into the substitutional A site and the preferential orientation (PV^V) of the PV_2 complex. Since the two crystallographically inequivalent sites are energetically equivalent in the crystal, the asymmetry may stem from the CVD growth of (111) diamond. However, dopant incorporation in the step-flow mode of film growth³¹ is a complicated process, and theoretical studies on P doped diamond are limited. Here, we discuss the information that can be obtained from the present result, as well as a possible scenario for the preferential orientation of the PVSVC. For component α , the difference in occupancy implies that the incorporation of P atoms at the A and B sites encounters different energy barriers during crystal growth. For component β , the preferential orientation may be related to the preferential incorporation of a substitutional P atom in the A site. In N-doped CVD (111) diamond, theoretical studies¹⁶ on N-V centres suggested preferential occupation of the A site during the step-flow mode of film growth, followed by the formation of vacancies leading to the [111]-oriented N-V centre. Herein we explained that the oriented N-V centre is formed because a lone pair of the N atom in the A site at the surface pointing to the vacuum increases the formation energy for another C atom located on top of the N atom. A similar mechanism can be considered for the formation of a PVSVC. However, the local structure of the PVSVC is different from that of the N-V centre, comprising a substitutional N atom and a vacancy on an adjacent lattice site^{12,14,15}. This suggests that the PV complex should transform to the PVSVC via structural relaxation, indicating that the mechanism of formation of PVSVC is more complicated. We hope

that this study motivates further theoretical studies to elucidate the atomistic mechanism of preferential orientation of the PVSVC.

In conclusion, we confirmed asymmetric P dopant incorporation, i.e. the preferential incorporation of P atoms into one of the two substitutional sites and the preferential orientation of the PVSVC. The chemical- and crystal-site sensitive local structures of dopants can shed light on the mechanism of doping and provide strategies to control the orientation of dopant-related complexes. In the current situation of PEH, public-use experimental stations that are equipped with computer controlled sample manipulators and wide-acceptance angle electron analysers have been developed in SPring-8, and a data analysis tool with many functions has also been developed, so that measurements become easier. These progresses have enabled PEH study on diluted samples, like present study, too. Such efforts are in progress, and will make PEH a more popular and powerful technique in materials science in near future.

Methods: A homoepitaxial heavily P-doped (111) diamond film was prepared by MPCVD³². n_p is $1 \times 10^{20} \text{ cm}^{-3}$ (0.06 at.%), as determined by secondary ion mass spectroscopy. The thickness of the P-doped layer is estimated to be $\sim 2 \text{ }\mu\text{m}$ using a relation between growth rate and growth time³³. Resistivity measurements showed a semiconducting temperature dependence and a value of $\sim 200 \text{ }\Omega \text{ cm}$ ($5 \times 10^{-3} \text{ Scm}^{-1}$) at $\sim 27 \text{ }^\circ\text{C}$. The film surface used for the PEH measurements was cleaned using H_2 plasma, and was therefore a H-terminated film. To reduce adsorbed molecules on the surface, the sample was annealed *in situ* at $\sim 500 \text{ }^\circ\text{C}$ for 10 min under ultrahigh vacuum before the measurements.

PEH measurements for C 1s and P 2p were performed at BL25SU, SPring-8, using a Scienta Omicron DA30 electron analyser with a photon energy of 700 eV (1.8 nm). The energy resolution was set to $\sim 170 \text{ meV}$ ($4.3 \times 10^{-4} \text{ nm}$). The probing depth of the present PEH is of the

order of 1 nm, as estimated from the inelastic mean free path of the photoelectron having kinetic energy ~ 500 eV. The base pressure of the measurement chamber was better than 5×10^{-8} Pa. The chemical potential of the sample was determined from the Fermi edge of a molybdenum substrate electrically contacted with the sample. All the measurements were performed at room temperature to prevent charging. A map of the photoelectron angular distribution, which is the photoelectron hologram, was acquired from a series of measured data (angular regions of $\pm 6^\circ$ and $\pm 10^\circ$) using the three-fold symmetry operation and mirror symmetry operation according to the symmetry of the (111) surface. 3D atomic images were reconstructed with the scattering pattern extraction algorithm using L_1 -linear regression (SPEA-L1)²³. Simulated photoelectron holograms were obtained using the TMSP code²³, with an atomic cluster of radius 3 nm and mean free path 1 nm, based on the calculated positions of P and C atoms. The site symmetry of the substitutionally incorporated P atoms used was T_d . Although this is different from the previously reported D_{2d} symmetry³⁵, the difference of local structure around a P atom between T_d and D_{2d} is small; hence, the simulated photoelectron hologram patterns may be identical (for detailed information on the PEH technique, see Supporting Information).

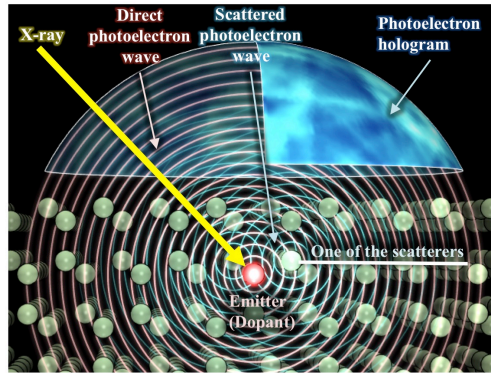


Figure 1. Illustration of photoelectron holography system.

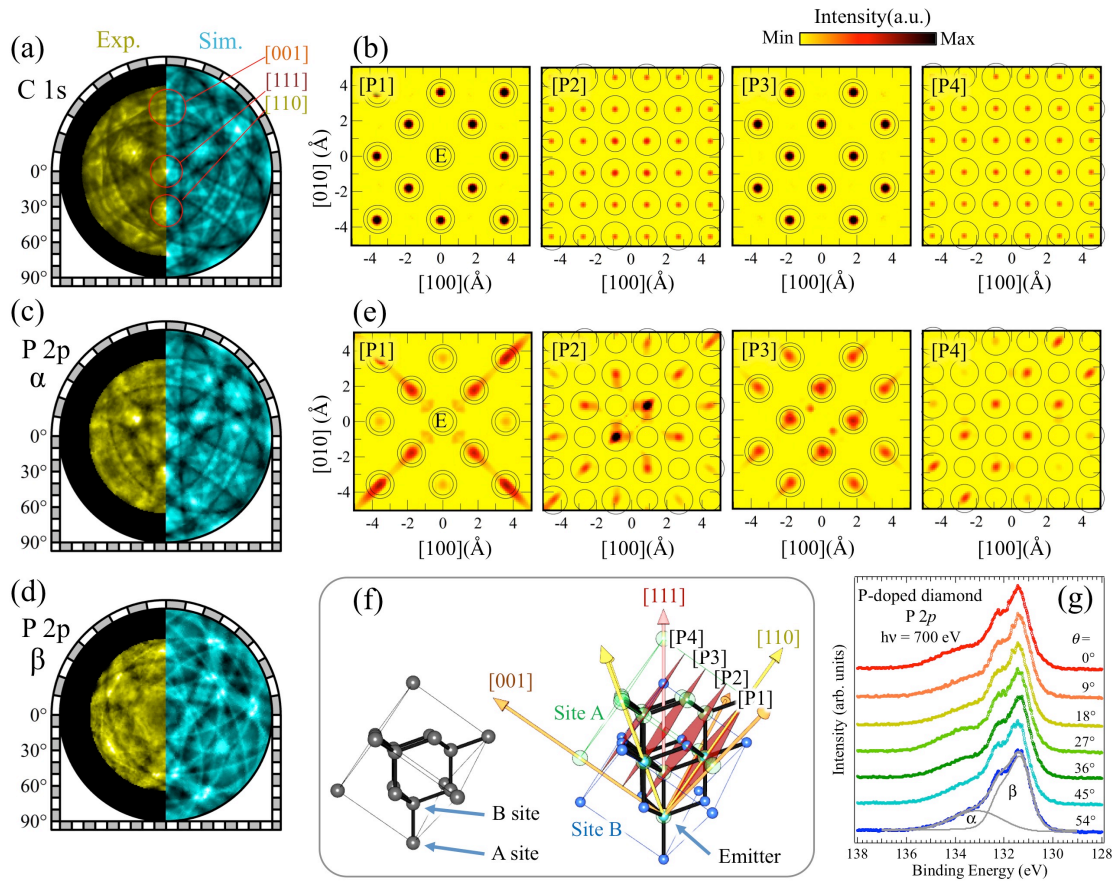


Figure 2. (a) Experimental (left) and simulated (right) images of C1s photoelectron hologram of P-doped diamond (111). The centre of the hologram corresponds to the [111] direction and the angle with respect to the centre represents the polar angle. (b) Slices of the reconstructed 3D atomic image from the observed hologram. Planes [P1-P4] in (b) correspond to the planes perpendicular to [001] at $z = 0, 0.89, 1.78,$ and 2.67 Å, respectively. Mark E indicates the photoelectron emitter. Large and small circles indicate the expected positions of carbon atoms as viewed from the A and B sites, respectively. (c) and (d) are the same as (a), but show P 2p holograms for components α and β , respectively. (e) is the same as (b), but for the component α of P 2p. (f) Diamond crystal structure (left) and a superposition of atomic structures, as viewed from the A and B sites as emitters (right). The observed hologram provides information from

both structures. (g) Angular dependence of the core-level spectra of P 2p with respect to the surface normal. The two components α and β are labelled.

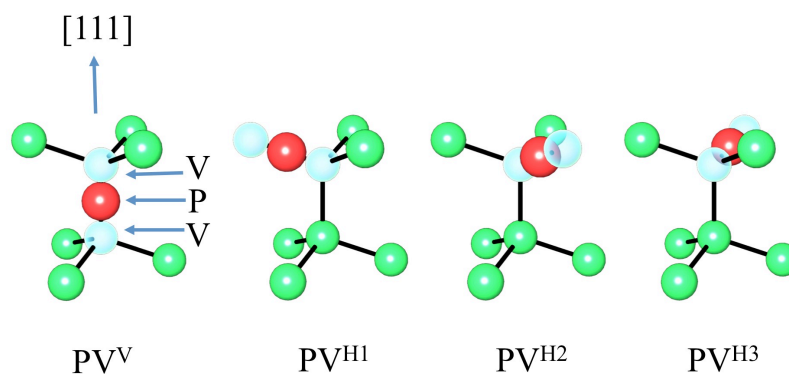


Figure 3. The structure of the PV split vacancy complex (PVSVC) in diamond. There are four candidate directions in diamond. Vertical PVSVC is denoted as PV^V and others are PV^{Hx} ($x = 1, 2, \text{ and } 3$).

ASSOCIATED CONTENT

Supporting Information. I. Simulated photoelectron holograms for substitutional P, PVSVC, and interstitial P, and II. details of PEH technique (file type: PDF).

AUTHOR INFORMATION

Corresponding Author

* T. Y. (yokoya@cc.okaym-u.ac.jp), * T. M. (matusita@spring-8.or.jp)

Present Addresses

K. Terashima, #National Institute for Materials Science, 1-2-1 Sengen, Tsukuba, Ibaraki 305-0047, Japan

Author Contributions

T.Y and K.T. planned the experiment. T.Y, K.T., A.T., T.F., H.F., T.M., and T.W. acquired the data. H.K. synthesized and characterized the sample. A.T and K.T. performed preliminary analyses, and T.M. analysed the data and prepared the figures. T.O. provided theoretical support for dopant local structures. T.Y., K.T., A.T., T.M., T.K., H.K., S.Y., T.O., T.W., Y.M., and T.M. discuss the results T.Y wrote the manuscript, with the help of T.M. and H.K.

Notes

The authors declare no competing financial interests.

ACKNOWLEDGMENT

We thank Y. Yano, T. Nagayama, M. Sunagawa, and W. Hosoda for their help with the photoelectron holography measurements at SPring-8 and analysis. We also thank Y. Nogami for valuable discussions. This work was supported by a Grant-in-Aid for Scientific Research of the Ministry of Education, Culture, Sports, Science and Technology, Japan (26105007, 26105013, 17H05220). The measurements at SPring-8 were performed under proposal numbers 2015A1144,

2016A1204, 2016B1352, 2017B1169, and 2018A1161. Preliminary measurements were performed at BL5, HiSOR, under the proposal number BL-5-15-A2.

REFERENCES

- (1) Bourgoin, J.; Lannoo, M. *Point Defects in Semiconductors II*; Springer-Verlag, Berlin Heidelberg, 1983; Chapters 3 and 4.
- (2) Wild, C.; Koidl, P.; Muller-Sebert, W.; Walcher, H.; Kohl, R.; Herres, N.; Locher, R.; Samlenski, R.; Brenn, R. Chemical vapour deposition and characterization of smooth {100}-faceted diamond films. *Diam. Relat. Mater.* **1993**, *2*, 158–168.
- (3) Koizumi, S.; Kamo, M.; Sato, Y.; Ozaki, H.; Inuzuka, T. Growth and characterization of phosphorous doped {111} homoepitaxial diamond thin films. *Appl. Phys. Lett.* **1997**, *71*, 1065–1067.
- (4) Isberg, J.; Hammersberg, J.; Johansson, E.; Wikstrom, T.; Twitchen, D. J.; Withhead, A. J.; Coe, S. E.; Scarsbrook, G. A. High Carrier Mobility in Single-Crystal Plasma-Deposited Diamond. *Science* **2002**, *297*, 1670–1672.
- (5) Achard, J.; Silva, F.; Tallaire, A.; Bonnin, X. Lombardi, G.; Hassouni, K.; Gicquel, A. High quality MPACVD diamond single crystal growth: high microwave power density regime. *J. Phys. D: Appl. Phys.* **2007**, *40*, 6175–6188.
- (6) Gracio, J. J.; Fan, Q. H.; Madaleno, J. C. Diamond growth by chemical vapour deposition. *J. Phys. D: Appl. Phys.* **2010**, *43*, 374017.

- (7) Yamada, H.; Chayahara, A.; Umezawa, H.; Tsubouchi, N.; Mokuno, Y.; Shikata, S. Fabrication and fundamental characterizations of tiled clones of single-crystal diamond with 1-inch size. *Diam. Relat. Mater.* **2012**, *24*, 29–33.
- (8) Nad, S.; Gu, Y.; Asmussen, J. Growth strategies for large and high quality single crystal diamond substrates. *Diam. Relat. Mater.* **2015**, *60*, 26–34.
- (9) Schreck, M.; Gsell, S.; Brescia, R.; Fischer, M. Ion bombardment induced buried lateral growth: the key mechanism for the synthesis of single crystal diamond wafers. *Sci. Rep.* **2017**, *7*, 44462.
- (10) Childress, L.; Gurudev Dutt, M. V.; Taylor, J. M.; Zibrov, A. S.; Jelezko, F.; Wrachtrup, J.; Hemmer, P. R.; Lukin, M. D. Coherent dynamics of coupled electron and nuclear spin qubits in diamond. *Science* **2006**, *314*, 281–285.
- (11) Balasubramanian, G.; et al. Ultralong spin coherence time in isotopically engineered diamond. *Nat. Mater.* **2009**, *8*, 383–387.
- (12) Doherty, M. W. The nitrogen-vacancy colour centre in diamond. *Phys. Rep.* **2013**, *528*, 1–45.
- (13) Edmond, A. M.; D’Haenens-Johansson, U. F. S.; Newton, M. E.; Fu, K.-M. C.; Santori, C.; Beausoleil, R. G.; Twitchen, D. J.; Markham, M. J. Production of oriented nitrogen-vacancy color centers in synthetic diamond. *Phys. Rev. B* **2012**, *86*, 035201.
- (14) Pham, L. M.; Bar-Gill, N.; Le Sage, D.; Belthangady, C.; Stacey, A.; Markham, M.; Twitchen, D. J.; Lukin, M. D.; Walsworth, R. L. Enhanced metrology using preferential orientation of nitrogen-vacancy centers in diamond. *Phys. Rev. B* **2012**, *86*, 121202(R).

- (15) Fukui, T.; et al. Perfect selective alignment of nitrogen-vacancy centers in diamond. *Appl. Phys. Exp.* **2014**, 7, 055201.
- (16) Miyazaki, T.; et al. Atomistic mechanism of perfect alignment of nitrogen-vacancy centers in diamond. *Appl. Phys. Lett.* **2014**, 105, 261601.
- (17) Ashcroft, N. W.; Mermin, N. D. *Solid State Physics*; Saunders College, Forthworth, 1976; p 76.
- (18) Berman, R. (editor), *Physical Properties of Diamond*; Oxford University Press, London.
- (19) Chu, W.-K.; Mayer, J. W.; Nicolet, M.-A., *Backscattering Spectrometry*; Academic Press, Inc., Orland, Florida, 1978; Chapter 8.
- (20) Teo, B. K. *EXAFS: Basic Principles and Data Analysis*; Berlin, Tokyo: Springer-Verlag, 1986.
- (21) Ishikawa, R.; Lupini, A. R.; Findlay, S. D.; Taniguchi, T.; Pennycook, S. J. Three-dimensional location of single dopant with atomic precision by aberration-corrected scanning transmission electron microscopy. *Nano Lett.* **2014**, 14, 1903–1908.
- (22) Barton, J. J. Photoelectron holography. *Phys. Rev. Lett.* **1988**, 61, 1356–1359.
- (23) Matsushita, T.; Matsui, F.; Daimon, H.; Hayashi, K. Photoelectron holography with improved image reconstruction. *J. Electron Spectrosc. Relat. Phenom.* **2010**, 178–179, 195–220.
- (24) Tsutsui, K.; et al. Individual atomic imaging of multiple dopant sites in as-doped Si using spectro-photoelectron holography. *Nano Lett.* **2017**, 17, 7533–7538.

- (25) Kato, Y.; Tsujikawa, D.; Hashimoto, Y.; Yoshida, T.; Fukami, S.; Matsuda, H.; Taguchi, M.; Matsushita, T.; Daimon, H. Three-dimensional atomic arrangement around active/inactive dopant sites in boron-doped diamond. *Appl. Phys. Exp.* **2018**, 11, 061302.
- (26) Kato, Y.; Matsui, F.; Shimizu, T.; Daimon, H.; Matsushita, T.; Guo, F. Z.; Tsuno, T. Dopant-site effect in superconducting diamond (111) studied by atomic stereophotography. *Appl. Phys. Lett.* **2007**, 91, 251914.
- (27) Okazaki, H.; et al. Multiple phosphorous chemical sites in heavily phosphorous-doped diamond. *Appl. Phys. Lett.* **2011**, 98, 082107.
- (28) Hasegawa, M.; Teraji, T.; Koizumi, S. Lattice location of phosphorous in n-type homoepitaxial diamond films grown by chemical-vapor deposition. *Appl. Phys. Lett.* **2001**, 79, 3068–3070.
- (29) Shikata, S.; Yamaguchi, K.; Fujiwara, A.; Tamenori, Y.; Yahiro, J.; Kunisu, M.; Yamada, T. X-ray absorption fine structure study of heavily P doped (111) and (001) diamond. *Appl. Phys. Lett.* **2017**, 110, 072106.
- (30) Jones, R.; Lowther, J. E.; Goss, J. Limitations to n-type doping in diamond: The phosphorus-vacancy complex. *Appl. Phys. Lett.* **1996**, 69, 2489–2491.
- (31) Tokuda, N.; Ogura, M.; Yamasaki, S.; Inokuma, T. Anisotropic lateral growth of homoepitaxial diamond (111) films by plasma-enhanced chemical vapor deposition. *Jpn. J. Appl. Phys.* **2014**, 53, 04H04.

- (32) Kato, H.; Umezawa, H.; Tokuda, N.; Takeuchi, D.; Okushi, H.; Yamasaki, S. Low specific contact resistance of heavily phosphorus-doped diamond film. *Appl. Phys. Lett.* **2008**, *93*, 20213.
- (33) Kato, H.; Makino, T.; Ogura, M.; Takeuchi, D.; Yamasaki, S. Maskless Selective Growth Method for p-n Junction Applications on (001)-oriented Diamond. *Jpn. J. Appl. Phys.* **2012**, *51*, 090118.
- (34) Yeh, J.J.; Lindau, I. Subshell Photoionization Cross Sections. *Atomic Data and Nuclear Data Tables* **1985**, *32*, 1–155.
- (35) Orita, N.; Nishimatsu, T.; Katayama-Yoshida, H. Ab initio study for site symmetry of phosphorous-doped diamond. *Jpn. J. Appl. Phys.* **2007**, *46*, 315–317.